AFRL-RX-WP-TR-2011-4133

TECHNICAL OPERATIONS SUPPORT III (TOPS III)

Task Order 0061: Fundamental Theory Based Assessment of Thermoelectric Merit Factor for Heusler Alloys

Alper Kinaci, Shiv Meka, Cem Sevik, and Tahir Cagin
Texas A&M University

OCTOBER 2010
FINAL REPORT

STINFO COPY

AIR FORCE RESEARCH LABORATORY
MATERIALS AND MANUFACTURING DIRECTORATE
WRIGHT-PATTERSON AIR FORCE BASE, OH 45433-7750
AIR FORCE MATERIEL COMMAND
UNITED STATES AIR FORCE

NOTICE AND SIGNATURE PAGE

Using Government drawings, specifications, or other data included in this document for any purpose other than Government procurement does not in any way obligate the U.S. Government. The fact that the Government formulated or supplied the drawings, specifications, or other data does not license the holder or any other person or corporation; or convey any rights or permission to manufacture, use, or sell any patented invention that may relate to them.

This report was cleared for public release by the USAF 88th Air Base Wing (88 ABW) Public Affairs Office and is available to the general public, including foreign nationals. Copies may be obtained from the Defense Technical Information Center (DTIC) (http://www.dtic.mil).

AFRL-RX-WP-TR-2011-4133 HAS BEEN REVIEWED AND IS APPROVED FOR PUBLICATION IN ACCORDANCE WITH ASSIGNED DISTRIBUTION STATEMENT.

*//SIGNATURE//_____
DOUGLAS DUDIS, Program Manager
Thermal Sciences and Materials Branch
Nonmetallic Materials Division

*//SIGNATURE//_____
NADER HENDIZADEH, Chief
Thermal Sciences and Materials Branch
Nonmetallic Materials Division

*//SIGNATURE//_____
SHASHI K. SHARMA, Deputy Chief
Nonmetallic Materials Division
Materials and Manufacturing Directorate

This report is published in the interest of scientific and technical information exchange, and its publication does not constitute the Government's approval or disapproval of its ideas or findings.

*Disseminated copies will show "//signature//" stamped or typed above the signature blocks.

REPORT DOCUMENTATION PAGE

Form Approved
OMB No. 074-0188

1. REPORT DATE (DD-MM-YYYY)	2. REPORT TYPE	3. DATES COVERED *(From – To)*
October 2010	Final	19 December 2008 – 18 December 2010

4. TITLE AND SUBTITLE
TECHNICAL OPERATIONS SUPPORT III (TOPS III)
Task Order 0061: Fundamental Theory Based Assessment of Thermoelectric Merit Factor for Heusler Alloys

5a. CONTRACT NUMBER
FA8650-05-D-5807-0061

5b. GRANT NUMBER

5c. PROGRAM ELEMENT NUMBER
62102F

6. AUTHOR(S)
Alper Kinaci, Shiv Meka, Cem Sevik, and Tahir Cagin

5d. PROJECT NUMBER
4084

5e. TASK NUMBER
1P

5f. WORK UNIT NUMBER
BT103100-A

7. PERFORMING ORGANIZATION NAME(S) AND ADDRESS(ES)
Texas A&M University
College Station, TX 77843-3122
For
Universal Technology Corporation
1270 N. Fairfield Road
Dayton, OH 45432-2600

8. PERFORMING ORGANIZATION REPORT NUMBER

9. SPONSORING / MONITORING AGENCY NAME(S) AND ADDRESS(ES)
Air Force Research Laboratory
Materials and Manufacturing Directorate
Wright-Patterson Air Force Base, OH 45433-7750
Air Force Materiel Command
United States Air Force

10. SPONSOR/MONITOR'S ACRONYM(S)
AFRL/RXBTC

11. SPONSOR/MONITOR'S REPORT NUMBER(S)
AFRL-RX-WP-TR-2011-4133

12. DISTRIBUTION / AVAILABILITY STATEMENT
Approved for public release; distribution is unlimited.

13. SUPPLEMENTARY NOTES
Report contains color. PAO Case Number: 88ABW-2011-3204; Clearance Date: 06 Jun 2011.

14. ABSTRACT
Intensive previous work (1950-1970) led to discovery of bulk Bi_2Te_3 and Sb_2Te_3 type heavy metal, low temperature thermoelectrics having dimensionless figure of merits (ZT's) in the vicinity of 1. Nonetheless, no material having marginally higher performance over Bi-Te and Sb-Te thermoelectrics can yet be commercialized. Moreover, these materials are not very practical due to scarcity of the elements, toxicity and decomposition-evaporation problems at elevated temperatures. Today, there are a number of promising ideas eliminate that can be realized through advanced synthesizing techniques, to increase ZT of more commonplace compounds such as clathrates, skutterudites, disordered heavy metal compounds, Half-Heusler allows and complex oxides.

15. SUBJECT TERMS
Half-Heusler alloys, thermoelectrics

16. SECURITY CLASSIFICATION OF:			17. LIMITATION OF ABSTRACT	18. NUMBER OF PAGES	19a. NAME OF RESPONSIBLE PERSON
a. REPORT	b. ABSTRACT	c. THIS PAGE	SAR	29	Douglas Dudis
UNCLASSIFIED	UNCLASSIFIED	UNCLASSIFIED			19b. TELEPHONE NUBER *(include area code)* (937) 255-9728

Standard Form 298 (Rev. 2-89)
Prescribed by ANSI Std. Z39-18

Approved for public release; distribution unlimited.

TABLE OF CONTENTS

LIST OF FIGURES

1.0 INTRODUCTION

The intensive work in 1950-1970 period had led to discovery of bulk Bi_2Te_3 and Sb_2Te_3 type heavy metal, low temperature thermoelectrics having dimensionless figure of merits (ZT's) in the vicinity of 1. Nonetheless, no material having marginally higher performance over Bi-Te and Sb-Te thermoelectrics can be commercialized yet. Moreover, these materials are not very practical due to scarcity of the elements, toxicity and decomposition-evaporation problems at elevated temperatures [1]. Today, there are a number of promising ideas eliminate that can be realized through advanced synthesizing techniques, to increase ZT of more commonplace compounds such as clathrates [2], skutterudites [3], disordered heavy metal compounds [4], Half-Heusler alloys [5] and complex oxides [6]

The performance of a device for such an application is generally defined by its figure of merit Z.

$$Z = \frac{\sigma S^2}{\kappa} \tag{1}$$

where σ is electrical conductivity, κ is thermal conductivity and S is the Seebeck coefficient (thermo-electromotive force – voltage gradient produced in a material due to temperature gradient when electrical current is zero). By multiplying with average temperature, ZT (dimensionless figure of merit) is obtained. It is customary to seek a ZT larger than 0.5 in a material order to consider it as thermoelectric. However, it is stated that a magnitude 3 or higher should be obtained to replace existing commercial appliances, such as compressor based refrigerators, with thermoelectric based systems [7].

As it is seen from the Eq. (1), a high ZT is associated with, low internal resistance to electric flow i.e. high electrical conductivity (σ), low thermal conductivity (κ), which produces a large temperature difference between the ends and a large thermopower (S), that is required to obtain high voltage. The main problem with the thermoelectric performance is the inter-dependence of σ, κ and S. This dependence is basically through carrier concentration. Thermal and electrical conductivity increases while Seebeck coefficient decreases with increasing carrier concentration.

Luckily, recent developments in material synthesizing and device production methods can realize several ideas for increasing thermoelectric performance. Optimizing carrier density and band gap width (at least 10 kT [8]) is one route. This is achievable through doping and alloying. On the other hand, thermal conductivity has an additional contribution from lattice conduction which must also be minimized. Over the years, several empirical rules were obtained for low thermal conductivity such as, the necessity of high average coordination numbers, large number of atoms in unit cell and high atomic masses in materials. In addition to these, there are also two relatively new and promising ideas exist to produce materials with low lattice thermal conductivity. One of them is the cake-like structures where a weakly bonded atom or molecule in the unit cell creates localized vibrational and rotational modes. This controlled disorder is believed to posses the phonon behavior of a glass and electronic conduction of a crystal. The interest in Half-Heusler alloys is resulted from this design. Secondly, low dimensional structures such as ultra-thin films, nanowires, superlattices etc. should have reduced $\kappa_{lattice}$ due to increased phonon scattering from interfaces depending on the phonon mean free path. However, it is shown that [9, 10] miniaturizing below some critical length also modifies electronic band structure which results in high ZT's [11].

The figure of merit measurement is not a hard task for a large sized bulk sample, yet, it can get quite complicated for extremely small structural features. In order to understand partial contribution of each constituent in ZT and the physical reasoning behind it for a specific configuration, theoretical evaluation is necessary. Then again, calculation of ZT is a formidable task and generally necessitates several approaches to be employed at the same time. Here, it is convenient to state some of these methods in two general headings, electronic and lattice contribution.

2.0 THEORY

2.1 Electronic Contribution

Several qualitative methods are presented in literature [4, 12-18]. The approximations in these studies are similar, if not same, when calculating figure of merit. Restraining ourselves to derivation of Scheidemantal et al.'s [12] work, the transport coefficients for an isotropic solid in the presence of electric field and thermal gradient are given in equations

$$\vec{J} = \underset{\sim}{\sigma}\vec{E} - \underset{\sim}{\aleph}\vec{\nabla}T \tag{2}$$

$$\vec{J}_Q = T\underset{\sim}{\aleph}\vec{E} - \underset{\sim}{\kappa}_0\vec{\nabla}T \tag{3}$$

where $\vec{J}, \vec{J}_Q, \vec{E}, \underset{\sim}{\sigma}, \vec{\nabla}T, T$ are electric current density, heat current density, electric field, electrical conductivity, temperature gradient and absolute temperature respectively. Underscore (~) symbol represents tensorial quantities. From the definition of the Seebeck coefficient, the following equation can be extracted for single components as

$$S = \frac{\aleph}{\sigma} \tag{4}$$

Electronic contribution to thermal conductivity (κ_{el}) can be defined as the heat current produced per unit temperature gradient when electrical current is zero, thus

$$\kappa_{el} = \kappa_0 - T\sigma S^2 \tag{5}$$

The electrical current can be defined by the group velocity approximation as below

$$\vec{J} = e\sum_{\vec{k}} f_{\vec{k}}\vec{\upsilon}_{\vec{k}} \tag{6}$$

In this equation e, $f_{\vec{k}}, \vec{\upsilon}_{\vec{k}}$ are the charge of the carriers, population of the quantum state at k and the group velocity associated with that state. Group velocity can be represented as the gradient of band structure in reciprocal space, so

$$\vec{\upsilon}_{\vec{k}} = \frac{1}{\hbar}\frac{\partial \varepsilon_{\vec{k}}}{\partial \vec{k}} \tag{7}$$

Another approach can be constructed by relating group velocity to momentum

$$\vec{\upsilon}_{\vec{k}} = \frac{1}{m}\vec{p}_{\vec{k}} = \frac{1}{m}\left\langle \psi_{\vec{k}} \middle| p \middle| \psi_{\vec{k}} \right\rangle \tag{8}$$

It is shown that both methods can be implemented in DFT successfully to obtain group velocity [12, 13]. Finally, a model is needed to bridge between transport coefficients and group velocity. Here, Boltzmann transport equation is introduced

$$\left.\frac{df_{\vec{k}}}{dt}\right|_{scattering} = \frac{\partial f_{\vec{k}}}{\partial t} + \vec{\upsilon}_{\vec{k}} \cdot \frac{\partial f_{\vec{k}}}{\partial \vec{r}} + \frac{e}{\hbar}\left(\vec{E} + \frac{1}{c}\vec{\upsilon}_{\vec{k}} \times \vec{H}\right) \cdot \frac{\partial f_{\vec{k}}}{\partial \vec{k}} \tag{9}$$

The terms on the right hand side are the drift terms in time, spatial and momentum space. The term on the left hand side is the change of population due to scattering events. Due to complexity of such events relaxation time approximation can be used

$$\left.\frac{df_{\vec{k}}}{dt}\right|_{scattering} = -\frac{f_{\vec{k}} - f_0}{\tau} \tag{10}$$

where τ is the relaxation time. $f_0(\varepsilon_{\vec{k}})$ is the Fermi distribution function for fermions in the absence of fields and $\varepsilon_{\vec{k}}$ represent state energies. Replacing the scattering term and assuming no magnetic field and temperature gradient (diffusional dependence), the population is given as

$$f_{\vec{k}} = f_0(\varepsilon_{\vec{k}}) + e\left(-\frac{\partial f_0}{\partial \varepsilon}\right)\tau_{\vec{k}}\vec{\upsilon}_{\vec{k}} \cdot \vec{E} \tag{11}$$

Using Eq. 2, 6 and 11 together, and noting that the population $f_0(\varepsilon_{\vec{k}})$ is same for $\vec{k}$ and $-\vec{k}$, leading to cancellation in the summation and zero net current flow, electrical conductivity can be written as

$$\sigma = e^2 \sum_{\vec{k}} \left(-\frac{\partial f_0}{\partial \varepsilon}\right)\vec{\upsilon}_{\vec{k}}\vec{\upsilon}_{\vec{k}}\tau_{\vec{k}} \tag{12}$$

Let ξ be defined as the transport distribution such that

$$\xi = \sum_{\vec{k}} \vec{\upsilon}_{\vec{k}}\vec{\upsilon}_{\vec{k}}\tau_{\vec{k}} \tag{13}$$

Then, by using scalar components of coefficients electrical conductivity, Seebeck coefficient and thermal conductivity can be written as

$$\sigma = e^2 \int \left(-\frac{\partial f_0}{\partial \varepsilon}\right)\xi(\varepsilon) d\varepsilon \tag{14}$$

$$S = \frac{ek_B}{\sigma}\int \left(-\frac{\partial f_0}{\partial \varepsilon}\right)\xi(\varepsilon)\frac{\varepsilon - \mu}{k_B T} d\varepsilon \tag{15}$$

$$\kappa_0 = {k_B}^2 T \int \left(-\frac{\partial f_0}{\partial \varepsilon}\right)\xi(\varepsilon)\left[\frac{\varepsilon - \mu}{k_B T}\right]^2 d\varepsilon \tag{16}$$

The equations written above are for single band only, so additional band index n should be added next to k index.

3.0 RESULTS

The following are the cell structures and transport data (obtained from the theory mentioned above) for the three selected binary alloys (Ni3Sn, NiZr and Zr5Sn3) between Ni-Sn, Ni-Zr and Sn-Zr. All have metallic properties conduction properties. In addition, we also present ternary NiSrZr (which comes out to be a semiconductor) transport data.

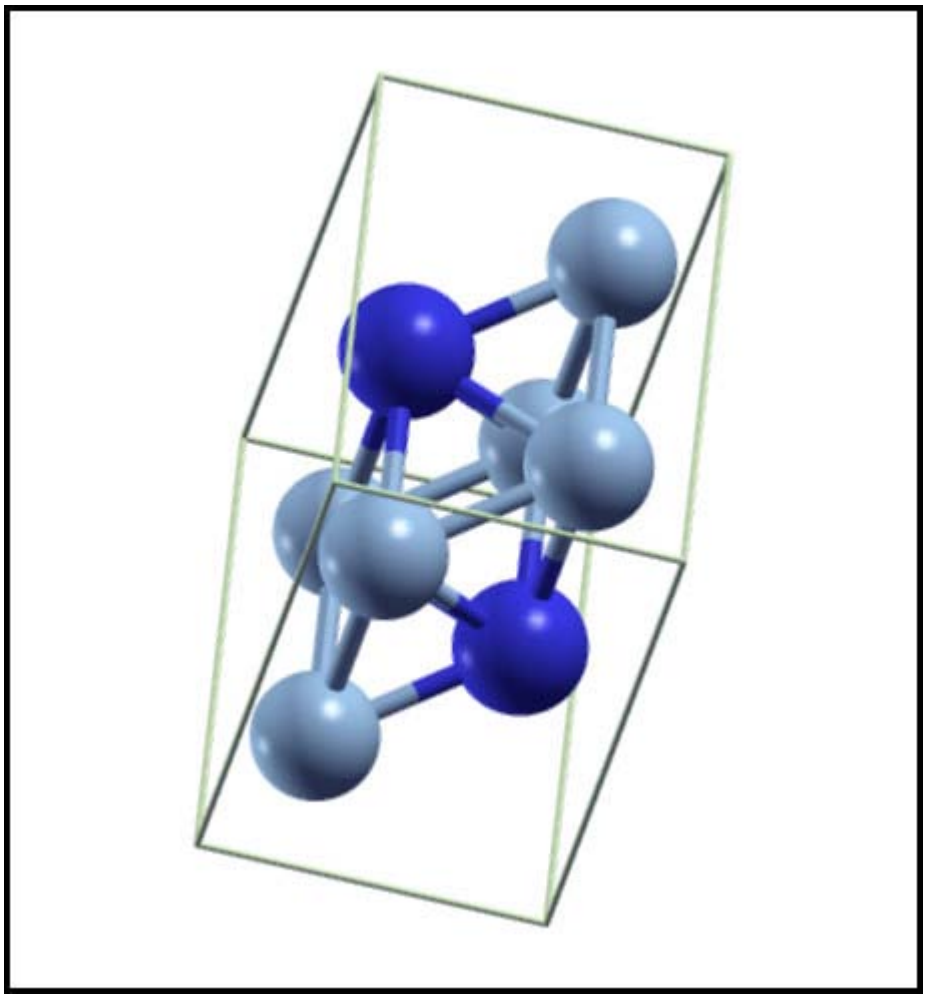

Figure 1. Ni3Sn (Hexagonal)

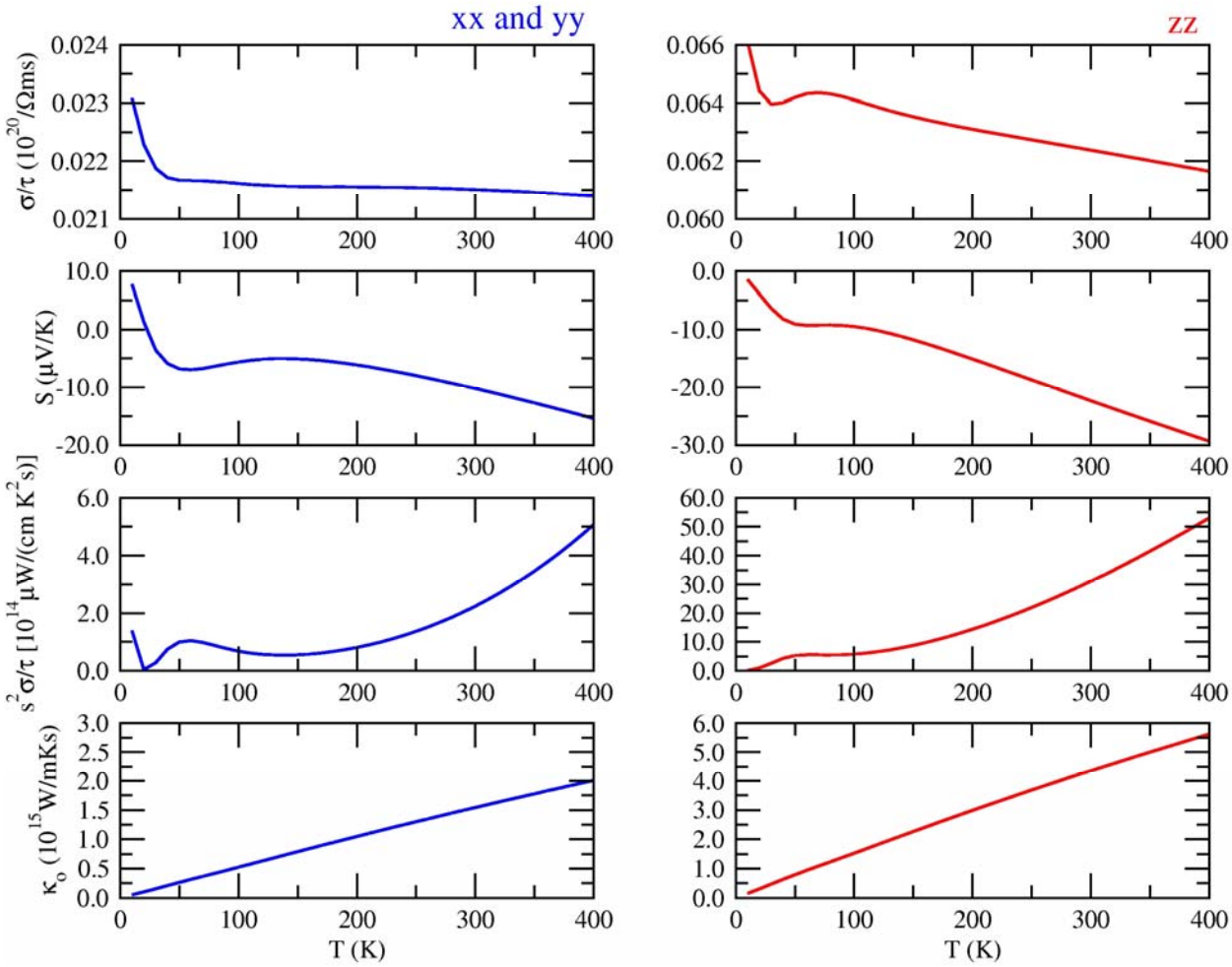

Figure 2. Ni3Sn Performance Data

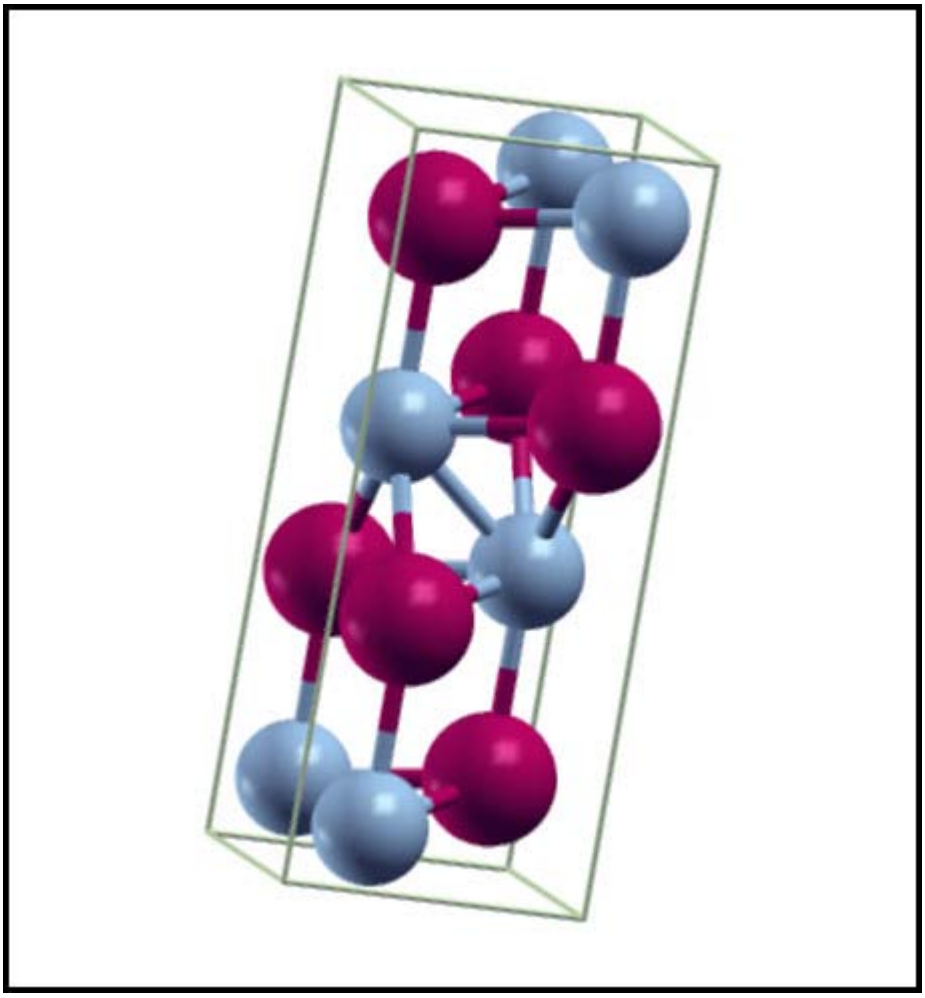

Figure 3. NiZr (Orthorhombic)

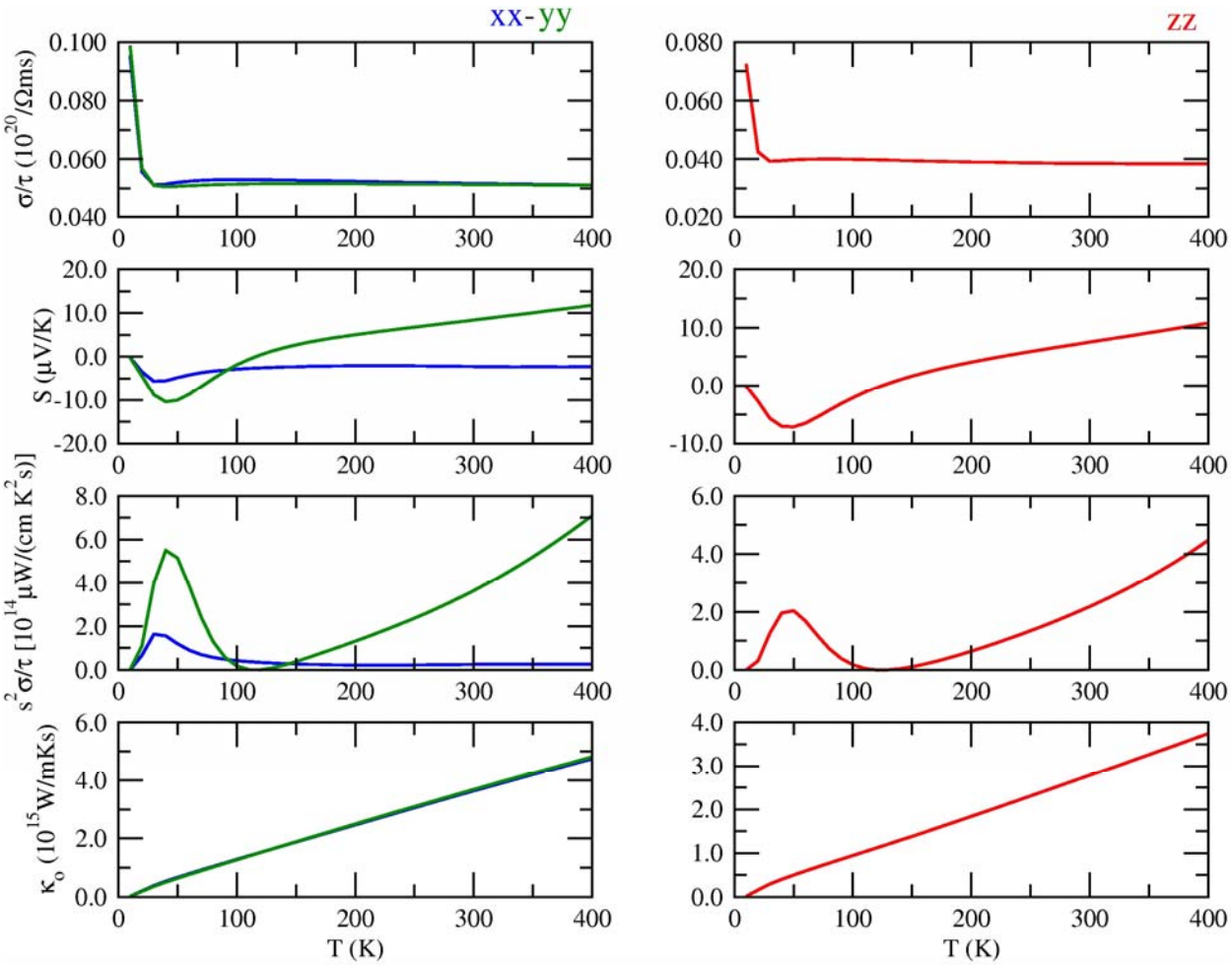

Figure 4. NiZr Performance Data

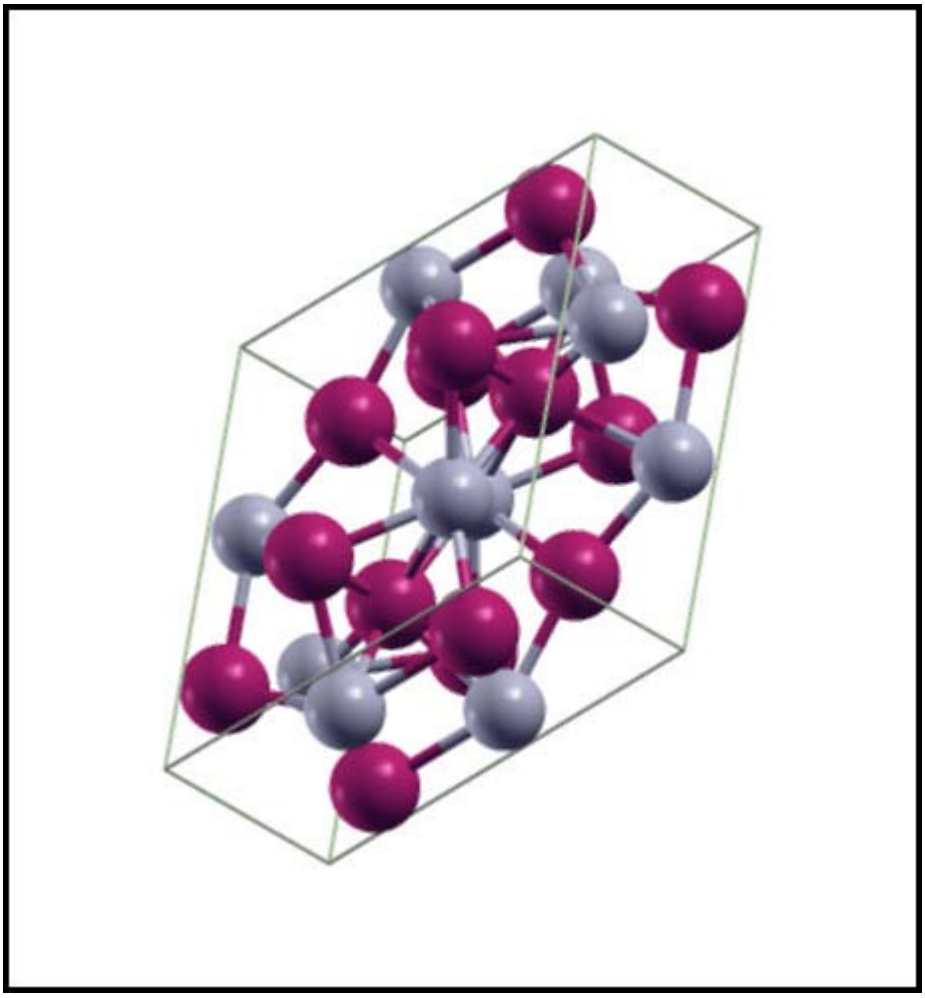

Figure 5. Zr5Sn3 (Hexagonal)

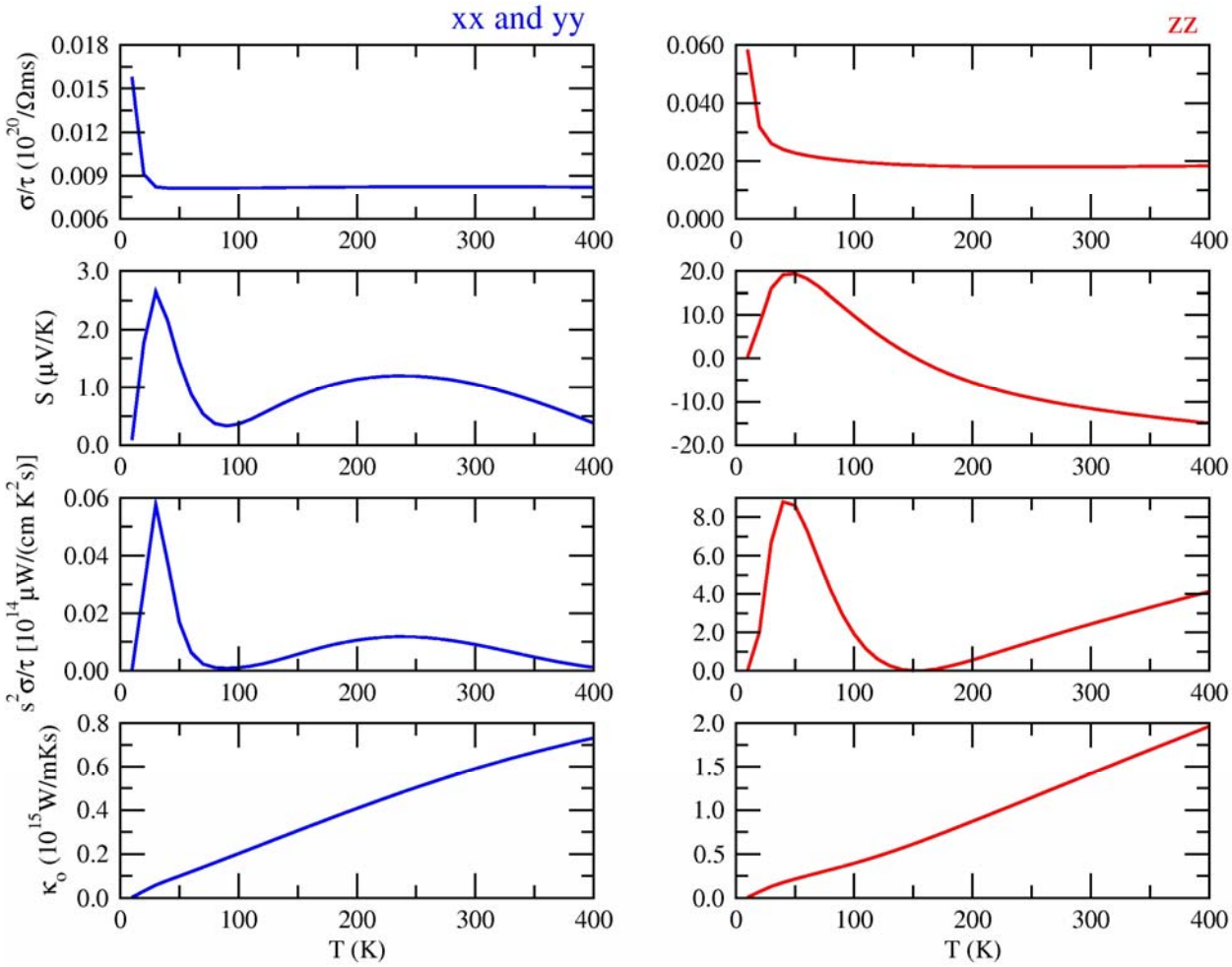

Figure 6. Zr5Sn3 Performance Data

Equilibrium structure of NiSrZn is found from equation of state. Secondly, the effect of hydrostatic pressure (volume contraction) on transport properties is shown.

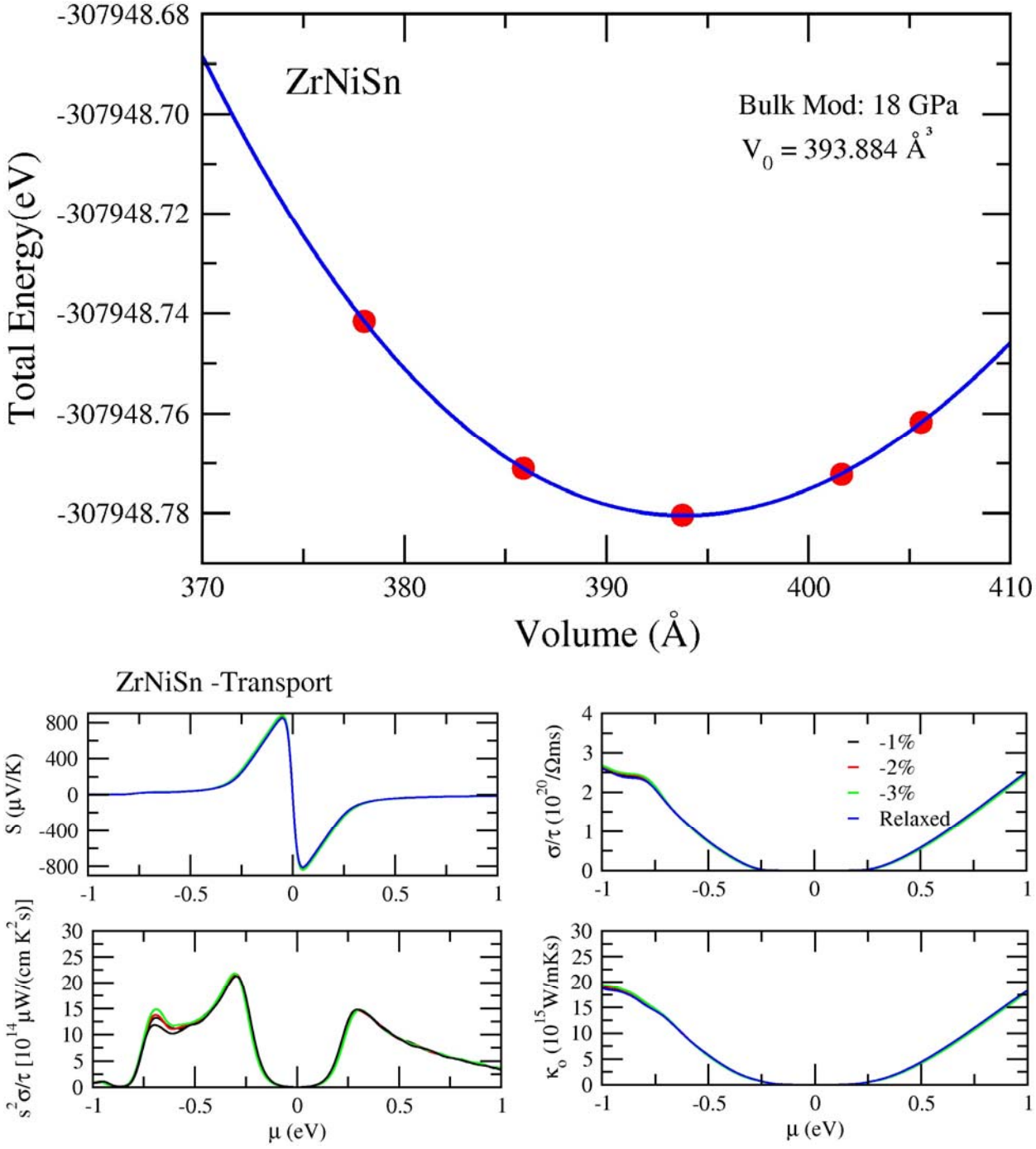

Figure 7. NiSrZn

4.0 HALF-HEUSLERS

Half-heuslers(HH) are Heusler *like* structures with half the atoms missing. Valence electron count (VEC) determines the electronic structure of Heusler[19] and HH structures[20]. VEC count of 18 implies existence of bandgap in HH[21]. HH are usually narrow bandgap semiconductors[a] that have moderate zT at high temperatures[22]. The important contributing factor to this "moderateness" is the thermal-conductivity (for eg. NiSnZr has *k* close to 10 W/m·K). But, their thermal conductivities are obviously lower than their Heusler counterparts. Tailoring the crystal could improve the thermal conductivity. For eg. in NiSnZr, Zr is replaced by a heavier Hf[23] and the thermoelectric conductivity was halved. The maximum zT in NiSnZr was found to be 0.7 (*fig.2.3*) which also happens to be an experimental prediction[23]. Most HH are n-type. It is still a challenge to find their **intrinsic** p-type and Si-Ge like alter ego. Asymmetry in the position of the Fermi level in the case of LaAlSi and CoSbTi implies they are a natural p-type alloys. In this study, four HH alloys were studied: i) CoSbTi ii) NiSnZr iii) LaAlSi and iv)NbFeSb

An ideal thermoelectric not only has a high zT. While three of the four observed structures performed well at 200 K (with zT ~ 0.75), counter intuitive to the generalized perception of zT in HH, NbFeSb has a high zT and behaves as a good thermoelectric over a wide temperature range and for a given doping concentration.

CoSbTi

From the functional form of the Seebeck coefficient, it is apparent that sharp DOS would lead to high S. These ternary inter-metallic structures resemble the MgAgAs cubic types. The transport coefficients of CoSbTi are fit to experiments (*fig.2.1*).

The doping concentration is estimated as 1.03E20 /cm^3. The bandgap was found to be: 0.98 eV (exp.:0.95). PBE functional was used for both exchange and correlation. The lattice parameters are almost the same as the experiment (deviation of 0.002%).

NiSnZr

NiSnZr is our first case where the use of LDA along with a fudge-factor "U" is necessary to prevent Mott-insulator[24, 25] behavior. The approximate exchange-correlation functional, no doubt, gives reasonable results for ground state energies, but fails in spelling out the proper electronic structure. Metallic behavior of the Half-filled d-shells is the prime reason for such an observation. In such cases, d-d Coulombic energies have to be taken into account and if one adds such a correction, the metallic behavior disappears. Is there a reasonable value of U to be added? Yes! "U", obviously depends on the orbital occupancy which means that the half-filled orbitals have less magnitude of U than the quarter-filled ones. One could make an educated guess and

[a] Take the case of NiSnZr, the bandgap is thanks to the hybridization of the d-shell electrons of Ni and p-electrons of Sn , and also contribution due to exchange splitting.

sweep U to match the lattice parameters or the electronic bandgap, OR a single-shot calculation needs the value of U be obtained from XPS[b,c,d]. It is apparent from *fig.2.3* that NiSnZr has a satisfactory max{zT} of 0.7 which agrees with the experimental prediction[23].

Computational details

The L(S)DAU parameters used are: U=7.52 and J=0.65. MHP grid of 26^3 was used. The deviation from experimental lattice parameters was close to 1%.

LaAlSi

Both the power factor and zT are to be kept in mind while deciding the overall performance of a dielectric. Since, Seebeck coefficients occurs as a squared value, one cannot rule out a possibility of a very high Seebeck and very low power factor exists. LaAlSi is a reasonably good thermoelectric for below 200 K applications (*fig.2.4*). This is apparent from the mean positions of the various Gaussian like zT vs T curves. At higher Ts, the electrons get thermally excited and nullify any voltage drop (because of narrow bandgap).

NbFeSb

Suprisingly, NbFeSb shows a good thermoelectric behavior for temperatures below 600K. There was minimal deviation in the calculated structural parameters when compared to the experimental ones obtained from ICSD. The bandgap was found to be 0.075 eV. A maximum zT was found to be 1.14. Carriers at the valence band have a small effective mass and thus making it possible for even the faintest of temperature gradients to populate the conduction band (which has a sharp band edge). Since the conduction band electrons are massive (from the DOS) and delocalized, possibility is that it develops reasonable potential (associated with the effective mass) and also has high-conductivity.

Computational details

There was minimal deviation between the experimental and the computed lattice parameters. LDA was used for both the exchange and correlation functional. 18^3 MHP grid was used from an SCF calculation which followed a 8^3 MHP relaxation[e].

Statement without proof: The difference between computed lattice parameters and the experimental values is minimal if one uses a primitive cell representation instead of the supercell.

---

[b] This exercise doesn't guarantee of exact lattice parameters as there are other shells that suffer from the lack of a better exchange-correlation functional.

[c] Ref. [31] deals with the extraction of U from XPS binding energies. In general, it is the effective (U-J) that needs to be corrected, J being the exchange correction which also depends on the occupancy since the exchange and correlation are a lumped unit in GGA/LDA.

[d] Occupancies needn't always be whole numbers as it would be shown in Chapter 3, the electron occupancies may even assume fractional values owing to hybridization of a particular state.

[e] Prior to calculating the SCF data values, it was made sure that all the systems saw through 1meV convergence both on k-points and the energies.

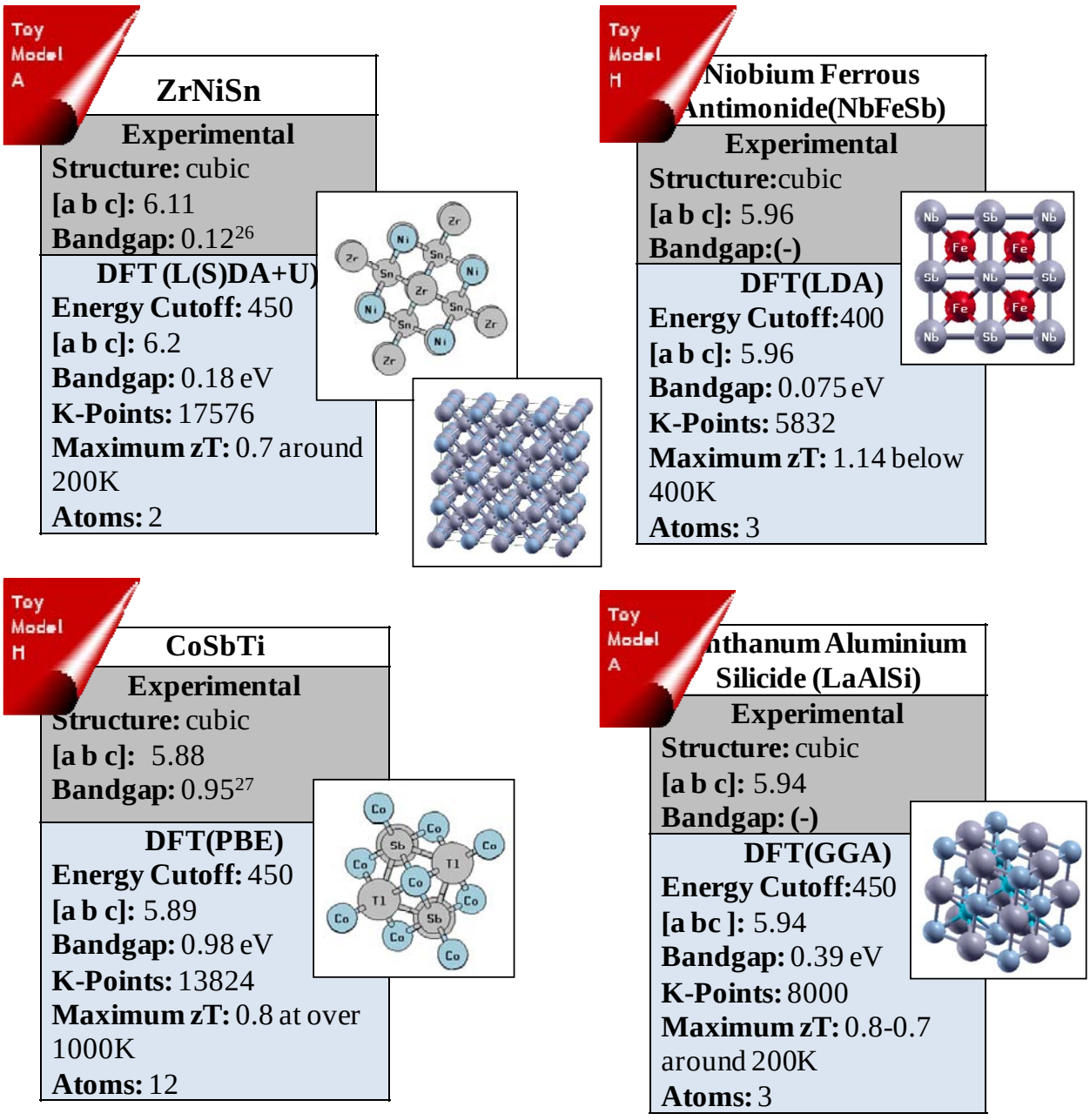

Figure 8. Summary of Lattice Parameters, Computational Parameters, and Band Gaps in HH

CoSbTi

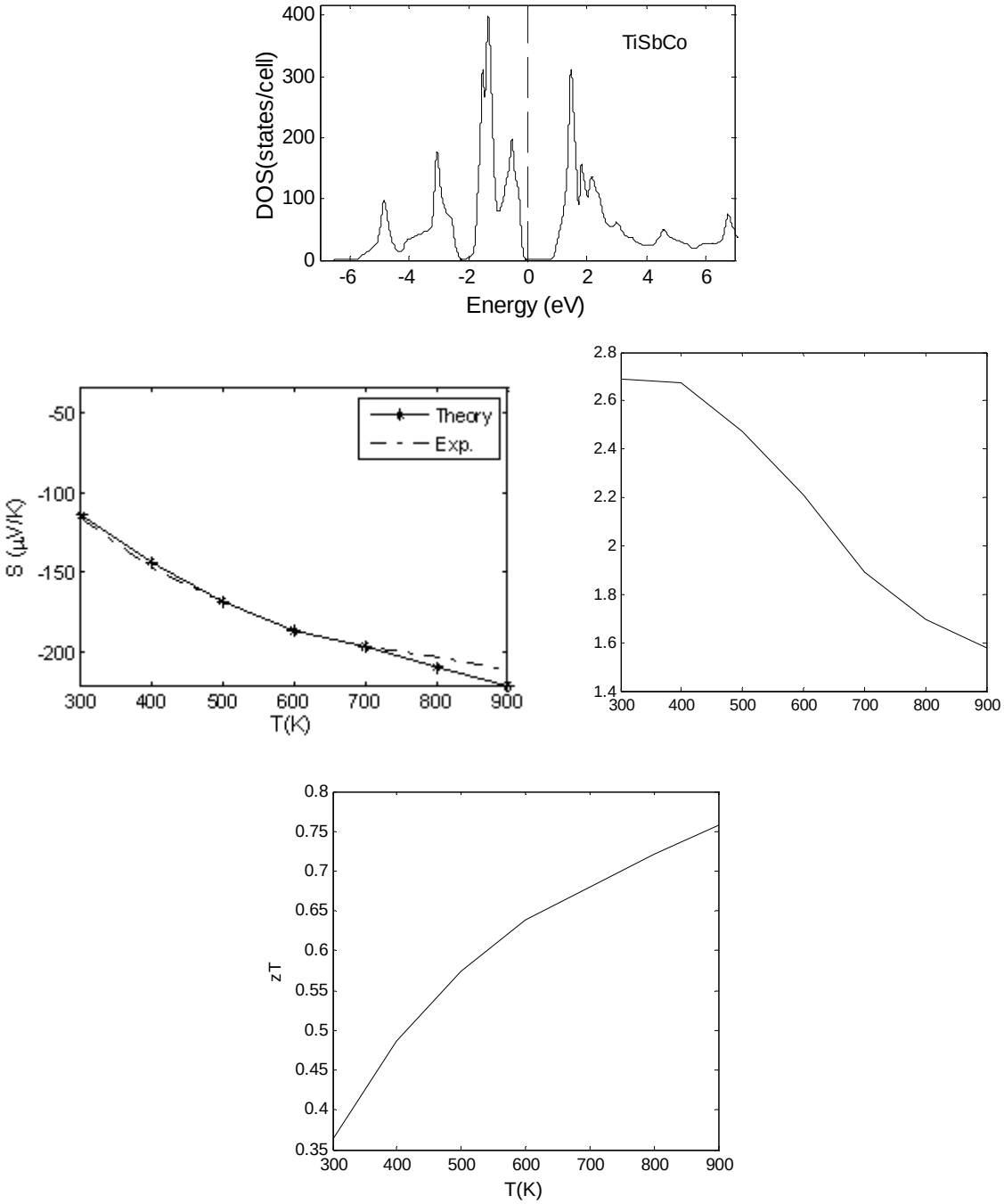

Figure 9. DOS, Experimental Fits to Compute Relaxation Time and zT

NiSnZr

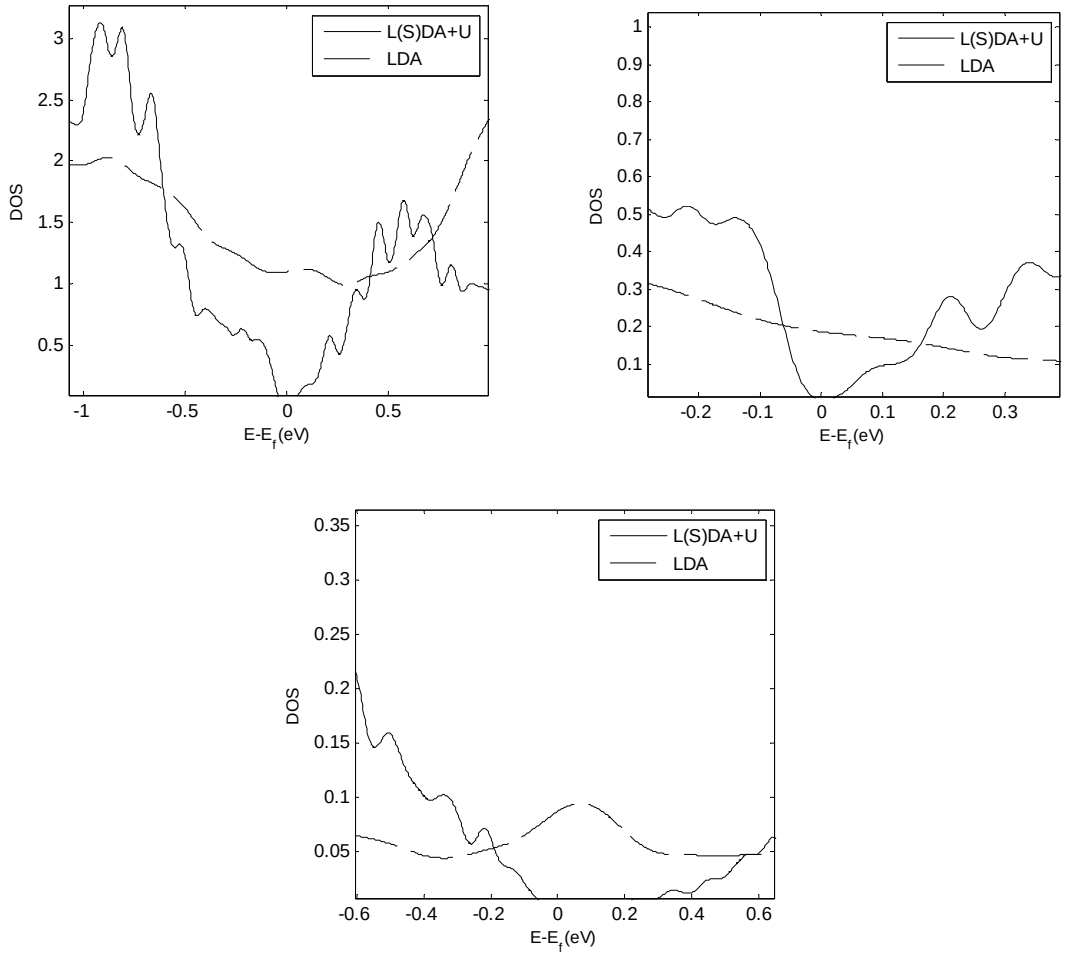

Figure 10. (Clockwise) i) Total-DOS of NiSnZr Calculated with the Two Methods - L(S)DA+U (U=7.5, J=0.65) and LDA. Basic Implementation of LDA Fails to Correctly Treat Correlation Effects in Highly Correlated Systems. Figure Also Compares Projected pDOS of Nickel in ii) t_2g and iii) eg States Using Both Methods

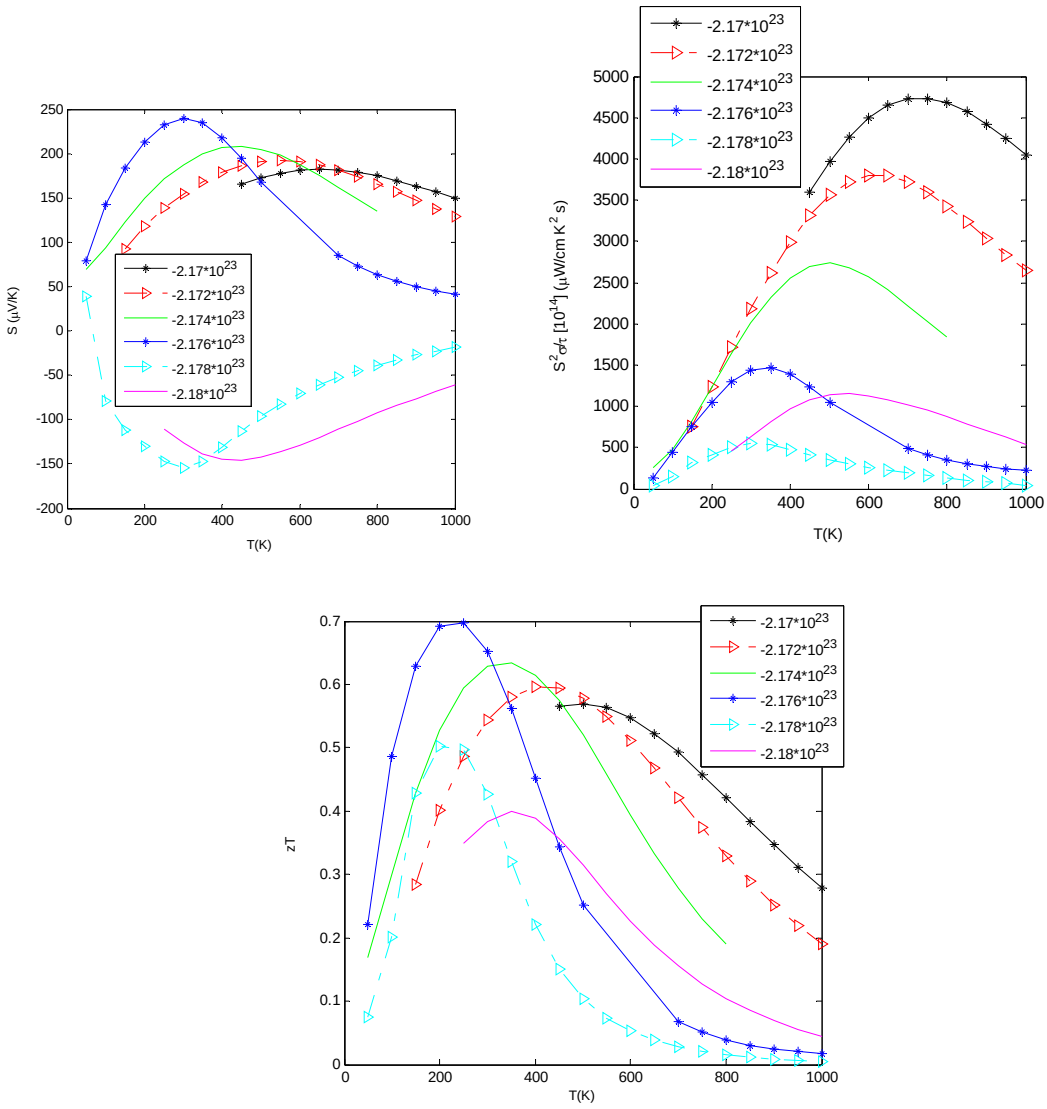

Figure 11. Seebeck Coefficient, Power Factor and ZT Plots of NiSnZr

LaAlSi

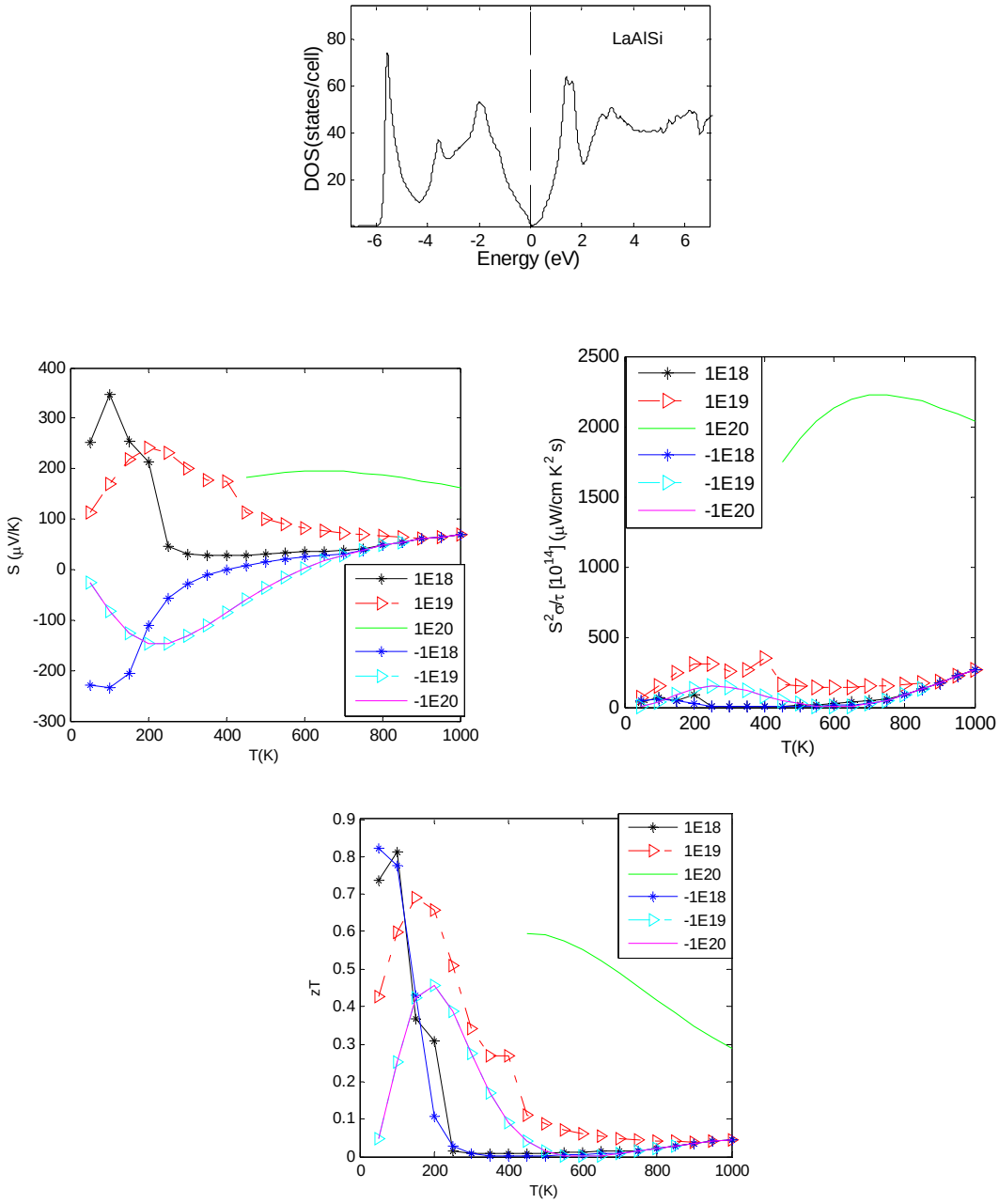

Figure 12. DOS, Seebeck Coefficient, Power Factor and ZT Plots of LiAlSi

NbFeSb

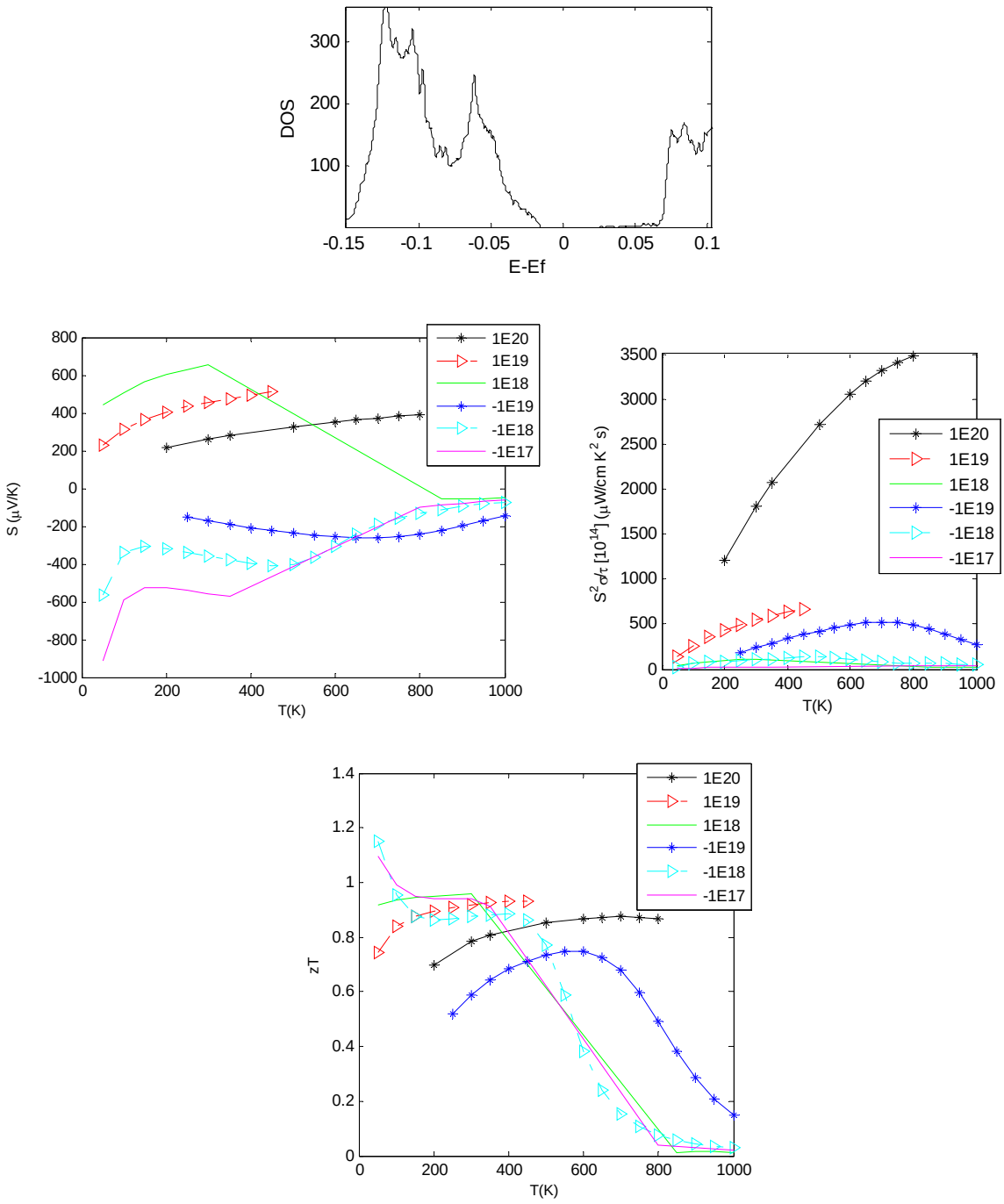

Figure 13. DOS, Seebeck Coefficient, Power Factor and ZT Plots of MbFeSb

The demand for energy is for sustainable development is increasing. One way to go about the problem is to *squeeze the fruit till the last drop.* Thermoelectrics do just this! They perform the last rites by scavenging waste heat. Car exhausts, geothermal energy, home heating, industries and microchips are sources where the systems get thermally equilibrated before being put to good use. Scavenger engineering has been one of the challenges of the recent past. A plethora of materials and alloys leads to confusion on rounding in on a material to be used as a thermoelectric. A rational approach would be to observe patterns of behavior of different classes of heat-scavengers and capture the physics to understand the rationale behind the working of these devices. Also, the quality of thermoelectric conversion has to be expressed in numbers so that one would be able to compare between two given samples, observe empirical patterns that could even help on improving the efficiency. Mathematically, the figure of merits (zT) sums it all: $zT=S^2\sigma T/k$ where S is the Seebeck coefficient which tells how much electrical work does a temperature gradient does, σ is the conductivity, T, the temperature and *k :* the thermal conductivity. While S is directly proportional to the open circuit voltage (developed across the structure that has just a temperature gradient without any external electric field ($\Delta V/\Delta T$)), the power factor ($pf\sigma$) is the closed circuit current and depends on the conductivity. In order to maximize the function zT, one needs to have both Seebeck coefficient and the electrical conductivity high, and *k* low. But this is contradicting. How can something develop a high *emf* and even pump current? The subtlety is: the overall product is what matters. But, it is a reasonable assumption since one needs not just a voltage difference developed, but the circuit ought to be closed or there could be charge buildup finally breaking the dielectric (joule heating). Beginning with thermocouples, thermoelectrics have a very long history. Thermoelectrics of the 70's aren't any better. Recent trends in nanostructured materials improved efficiency 4 folds.

Doping:

Type of carriers involved in the transport plays a crucial role in determining the efficiency of a thermoelectric. In general, it is advised to have higher concentration of carriers of one type. Bipolar carrier recombination adds to *k* which degrades the performance of the thermoelectric. And, therefore, one carrier type must dominate in order to have maximum S. Mixed conduction cancels out the net effect of charge flow as one carrier moves to the hot end and the other to the cold.

kappa "k"

According to Wiedemann-Franz law: $k=k_e+k_l$ where k_e is the electronic contribution (Lorentz factor $L=2.4\times10^{-8}\ J^2\ K^{-2}\ C^{-2}$) because of charge carriers transporting heat and k_l is the thermal conductivity due to phonons. For most systems, k_l has an above 75% contribution to the total *k*, and is mostly constant with concentration. Glasses are known for low k_l[a]. But, electrons in glasses are scattered making them poor thermoelectrics.

Low or High m*?

From simple Drude's model, large m* means good S but a bad σ. So, mobility is an important deciding factor in thermoelectric design. m* is directly proportional to the density of states. Flat bands (large m*) mean localized electrons and have a high S. Dephasing issues and lattice thermal conductivity, scattering, and anisotropy are a summed up contribution in the overall performance. Large m* with low conductivity (for eg.:chalcogenides) are a result of small

electronegativity differences while small m* and large conductivity are a result of large electronegativity differences, but both have a good zT.

Final Verdict

One needs a "phonon-glass and an electron crystal"[1] to realize a close to ideal thermoelectric. Glass like properties are achieved by scattering phonons, engineering scattering centers and making solid-solutions. Clathrates, filled skutterudites, Quantum dot super-lattices (QDSLs), Zintl phases have so far been identified as potential candidates in the high-zT region of thermoelectric operation. Nanostructuring and organic-inorganic hybrid structures may present other avenues to achieve goal of high ZT .

5.0 REFERENCES

[1] Ohta H., Kim S., Mune Y., Mizoguchi T., Nomura K., Ohta S., Nomura T., Nakanishi Y., Ikuhara Y., Hirano M., Hosono H. and Koumoto K., Nat. Mater., **6**, 129 (2007)

[2] Bentien A., Christensen M., Bryan J.D., Sanchez A., Paschen S., Steglich F., Stucky G.D. and Iversen B.B., Phys. Rev. B, **69**, 045107 (2004)

[3] Sales B.C., Mandrus D. and Williams R.K., Science, **272**, 1325 (1996)

[10] Snyder G.J., Christensen M., Nishibori E., Caillat T. and Iversen B.B., Nat. Mater., **3**, 468 (2004)

[4] Madsen G.K.H., J. Am. Chem. Soc., **128**, 12140 (2006)

[5] Muta H., Kurosaki K. and Shinsuke Y., J. Alloys Compd., **368**, 22 (2004)

[6] Cuong D.D., lee B., Choi K.M., Ahn H.S., Han S. and Lee J., Phys. Rev. Lett., **98**, 115503 (2007)

[7] Mahan G., Sales B. and Sharp J., Physics Today, **50**, 3, 42 (1997)

[8] Mahan G.D., J. Appl. Phys., **65**, 4, 1578 (1989)

[9] Hicks L.D. and Dresselhaus M.S., Phys. Rev. B, **47**, 19, 12727 (1993)

[10] Hicks L.D., Harman T.C., Sun X. and Dresselhaus M.S., Phys. Rev. B, **53**, 16, R10493 (1996)

[11] Venkatasubramanian R., Siivola E., Colpitts T. and O'Quinn B., Nature, **413**, 597 (2001)

[12] Scheidemantel T.J., Draxl C.A., Thonhauser T., Badding J.V. and Sofo J.O., Phys. Rev. B, **68**, 125210 (2003)

[13] Madsen G.K.H. and Singh D.J., Computer Physics Communications, **175**, 67 (2006)

[14] Zhang R., Wang C., Li J., Zhang J., Zhao M., Liu J., Zheng P., Zhang Y. and Mei L., arXiv:0809.0775v1 (2008)

[15] Chaput L., Pecheur P., Tobola J. and Scherrer H., Phys. Rev. B, **72**, 085126 (2005)

[16] Gao X., Uehara K., Klug D.D., Patchkovskii S., Tse J.S. and Tritt T.M., Phys. Rev. B, **72**, 125202 (2005)

[17] Yang J., Li H., Wu T., Zhang W., Chen L. and Yang J., Adv. Funct. Mater., **18**, 1 (2008)

[18] Mahan G.D. and Sofo J.O., Proc. Natl. Acad. Sci., **93**, 7436 (1996)

[19] G. S. Nolas, D. T. Morelli, and T. M. Tritt, Annual Review of Materials Science **29**, 89 (1999).

[20] C. Kittel, Thermal physics (Wiley, New York,, 1969).

[21] D. Jena, A. C. Gossard, and U. K. Mishra, Applied Physics Letters **76**, 1707 (2000).

[22] J. Androulakis, et al., J Am Chem Soc **129**, 9780 (2007).

[23]Y. Gelbstein, Z. Dashevsky, and M. P. Dariel, Physica B-Condensed Matter **363**, 196 (2005).

[24] P. F. P. Poudeu, J. D'Angelo, H. J. Kong, A. Downey, J. L. Short, R. Pcionek, T. P. Hogan, C. Uher, and M. G. Kanatzidis, J Am Chem Soc **128**, 14347 (2006).

[25] Y. Zhang, X. Z. Ke, C. F. Chen, J. Yang, and P. R. C. Kent, Phys Rev B **80** (2009).

[26] C. M. Fang, R. A. de Groot, and G. A. Wiegers, Journal of Physics and Chemistry of Solids **63**, 457 (2002).

[27] C. M. Bhandari and D. M. Rowe, Thermal conduction in semiconductors (Wiley, New York, 1988).

[28] M. Ferhat and J. Nagao, J Appl Phys **88**, 813 (2000).

[29] M. Schluter, G. Martinez, and M. L. Cohen, Phys Rev B **12**, 650 (1975).

[30] H. J. Monkhorst and J. D. Pack, Phys Rev B **13**, 5188 (1976).

[31] M. C. S. Kumar and B. Pradeep, Semicond Sci Tech **17**, 261 (2002).

[32] D. Y. Chung, T. Hogan, P. Brazis, M. Rocci-Lane, C. Kannewurf, M. Bastea, C. Uher, and M. G. Kanatzidis, Science **287**, 1024 (2000).

[33] G. F. Wang and T. Cagin, Phys Rev B **76** (2007).

[34] A. Lipovskii, et al., Appl Phys Lett **71**, 3406 (1997).

[35] N. Piccioli, J. M. Besson, and Balkansk.M, J Phys Chem Solids **35**, 971 (1974).

[36] T. Kyratsi, J. S. Dyck, W. Chen, D. Y. Chung, C. Uher, K. M. Paraskevopoulos, and M. G. Kanatzidis, J Appl Phys **92**, 965 (2002).

LIST OF SYMBOLS, ABBREVIATIONS, AND ACRONYMS

Acronym	Description
AFRL	Air Force Research Laboratory
DOD	Department of Defense
DTIC	Defense Technical Information Center
EAR	Export Administration Regulation
HH	Half-Heuslers
ITAR	International Traffic in Arms Regulation
LaAlSi	Lanthanum Aluminum Silicide
NbFeSb	Niobium Ferrous Antimonide
QDSLs	Quantum Dot Super-Lattices
RX	Materials
RXB	Nonmetallic Materials Division
RXBTC	Active Thermal Control Section
TOPS	Technical Operations Support
USAF	United States Air Force
VEC	Valence Electron Count
WPAFB	Wright-Patterson Air Force Base
ZT’s	Figure of Merits